Chemistry Europe
European Chemical Societies Publishing

WILEY VCH

Excellence in Chemistry Research

Announcing our new flagship journal

- Gold Open Access
- Publishing charges waived
- Preprints welcome
- Edited by active scientists

Meet the Editors of *ChemistryEurope*

Luisa De Cola
Università degli Studi di Milano Statale, Italy

Ive Hermans
University of Wisconsin-Madison, USA

Ken Tanaka
Tokyo Institute of Technology, Japan

ChemSusChem

Research Article
doi.org/10.1002/cssc.202300421

Chemistry Europe
European Chemical Societies Publishing

www.chemsuschem.org

Influence of Residual Water Traces on the Electrochemical Performance of Hydrophobic Ionic Liquids for Magnesium-Containing Electrolytes

Omar W. Elkhafif,[a] Hagar K. Hassan,[a, b, c] Maximilian U. Ceblin,[a] Attila Farkas,[a] and Timo Jacob*[a, b, c]

A trace amount of water is typically unavoidable as an impurity in ionic liquids, which is a huge challenge for their application in Mg-ion batteries. Here, we employed molecular sieves of different pore diameters (3, 4, and 5 Å), to effectively remove the trace amounts of water from 1-methyl-1-propylpiperidinium bis(trifluoromethylsulfonyl)imide (MPPip-TFSI) and 1-butyl-1-methylpyrrolidinium bis(trifluoromethylsulfonyl)imide (BMP-TFSI). Notably, after sieving (water content $<1\ mg\cdot L^{-1}$), new anodic peaks arise that are attributed to the formation of different anion-cation structures induced by minimizing the influence of hydrogen bonds. Furthermore, electrochemical impedance spectroscopy (EIS) reveals that the electrolyte resistance decreases by ~10% for MPPip-TFSI and by ~28% for BMP-TFSI after sieving. The electrochemical Mg deposition/dissolution is investigated in MPPip-TFSI/tetraglyme (1:1) + 100 mM $Mg(TFSI)_2$ + 10 mM $Mg(BH_4)_2$ using Ag/AgCl and Mg reference electrodes. The presence of a trace amount of water leads to a considerable shift of 0.9 V *vs.* Mg^{2+}/Mg in the overpotential of Mg deposition. In contrast, drying of MPPip-TFSI enhances the reversibility of Mg deposition/dissolution and suppresses the passivation of the Mg electrode.

Introduction

Magnesium-ion batteries are of growing interest to replace lithium (Li)-ion batteries due to the multi-valent character of Mg^{2+}, high volumetric capacity (3833 $mAh\cdot cm^{-3}$), affordability, and natural abundance of magnesium. Furthermore, Mg deposition/dissolution is achievable without the critical risk of a thermal runaway induced by dendrite formation.[1–3] However, the development of effective electrolytes for reversible Mg deposition/dissolution is a major challenge in realizing competitive Mg-ion batteries. Any suitable electrolyte for Mg deposition/dissolution must possess a wide electrochemical window stability, compatibility with both anode and cathode, as well as good ionic conductivity.[4]

So far, various electrolytes have been developed for reversible Mg deposition/dissolution, such as Grignard-based electrolytes,[5] boron-based electrolytes,[6,7] magnesium aluminate chloride-based electrolytes,[8] $Mg(TFSI)_2$-based electrolytes[9,10] and organometallic-based complex salt electrolytes.[11,12] For preparing these electrolytes, non-aqueous solvents such as ethers, carbonates, glymes, and ionic liquids are commonly used.[13] Among them, ionic liquids are of particular interest due to their merits including high ionic conductivity, electrochemical stability, non-flammability, low volatility, non-corrosive nature, wide electrochemical window, and good thermal stability.[14] Nevertheless, ionic liquids can be easily contaminated by water due to their hygroscopic nature.

The presence of water, even at low concentrations strongly influences the physical characteristics, structure, and dynamics of ionic liquids.[15] Various studies in the literature focus on the nature of interactions between ionic liquids and water, since investigating water-ionic liquid mixtures is of practical importance. It has been shown that the anionic counterpart plays a dominant role in the affinity of ionic liquids towards water due to its ability to form a hydrogen bond with the adsorbed water molecules.[16,17] The main interactions responsible for the solvation of water molecules in the ionic liquid are electrostatic, van der Waals, dipole-dipole interactions,[18,19] and the formation of hydrogen bonds.[16,17] Water molecules can form hydrogen bonds with either the cation or the anions and thus, influence the solvation behavior and orientation of ionic liquids, where a trace amount of water influences the complex interaction between anion and cation solvation mechanism.[20,21] However, the structure of ionic liquid-water mixtures is still poorly understood. Regarding the structure and behavior of the residual water molecules in ionic liquids, there are three

[a] O. W. Elkhafif, Dr. H. K. Hassan, Dr. M. U. Ceblin, Dr. A. Farkas, Prof. Dr. T. Jacob
Institute of Electrochemistry
Ulm University
Albert-Einstein-Allee 47, 89081 Ulm (Germany)
E-mail: timo.jacob@uni-ulm.de

[b] Dr. H. K. Hassan, Prof. Dr. T. Jacob
Helmholtz Institute Ulm (HIU) – Electrochemical Energy Storage
Helmholtzstr. 11, D-89081 Ulm (Germany)

[c] Dr. H. K. Hassan, Prof. Dr. T. Jacob
Karlsruhe Institute of Technology (KIT)
P.O. Box 3640, D-76021 Karlsruhe (Germany)

Supporting information for this article is available on the WWW under https://doi.org/10.1002/cssc.202300421

contradictory hypotheses. Accordingly, the residual water molecules can be either (i) separated from each other, and thus can interact strongly with the ions throughout the medium, (ii) undergo self-association or forming clusters, or (iii) weaken ion-ion interactions.[22] Additionally, water influences the phase behavior and the local structure of ionic liquids, resulting in a new hydrogen bond configuration and new features as was shown by Raman and infrared spectroscopy, as well as differential scanning calorimetry investigations.[23] Regarding the electrochemical stability and performance of ionic liquids, the electrolysis of water molecules occurs at potentials lower than the potential of the ionic liquid decomposition, generating H^+ and OH^- ions. These ions react with the ionic liquid, leading to a change in its chemical composition.[24] Additionally, water electrolysis dramatically narrows the electrochemical stability regime of ionic liquids by more than 2.0 V.[25] The stability of the electrode might decrease with increasing water content since water triggers cathodic corrosion of metal electrodes at relatively high negative potentials (similar to the potentials required for Mg deposition) in presence of non-reducible cations.[26] Additionally, the presence of water in the ionic liquid has a strong effect on the double-layer capacitance (C_{dl}) and its structure, consequently, the kinetic parameters of electroactive species at the electrochemical interface are altered.[24,27] With regard to their performance for Mg deposition/dissolution, a passivation layer of MgO and $Mg(OH)_2$ is typically formed due to a contamination of the ionic liquid with trace amounts of water, resulting in blocking and fading the conduction of Mg^{2+} ions.[28] Moreover, the presence of traces of water hinders their applicability for Mg deposition/dissolution with high reversibility and cyclic stability.[15,29] Thus, drying the ionic liquid is a crucial step to minimize the water content considerably, in other words, obtaining (almost) water-free ionic liquids.

Several treatments were employed for drying ionic liquids to achieve a very low water content. For instance, the combination of active carbon and silicates,[30] molecular sieves,[31–33] and different additives based on Mg salts, for example, diorganomagnesium species ($MgBu_2$), $MgCl_2$, borohydrides,[32] hexamethyldisilazane(HDMS),[34] dimethoxypropane (DMP)[35] and crown ethers such as 18-crown-6[35] were used as water scavengers. Furthermore, vacuum drying of ionic liquids[36] at around 100 °C using a vacuum pump ($< 10^{-3}$ mbar),[37] or a turbomolecular pump ($< 10^{-7}$ mbar) has also been reported.[38,39]

Among these different attempts, molecular sieves are promising candidates as water scavengers for the selective removal of water traces.[40] They are three-dimensional microporous inorganic hybrid materials in which their pore size can be easily tuned by altering the elemental composition (the added elements with different atomic radii).[41] The 4 Å molecular sieve is composed of silicates, aluminates, and Na_2O. The exchange of Na_2O with K_2O reduces the pore size to 3 Å. However, to increase the pore size to 5 Å, CaO can be used to replace Na_2O.[42]

The influence of trace amounts of water on the electrochemical behavior of ionic liquids is currently not investigated, despite the various implications and complications resulting from water within the ionic liquids mentioned above. Therefore, in the present work we studied (as model system) the electrochemical Mg deposition/dissolution from ionic liquid/tetraglyme system before and after drying. Therefore, in this contribution, we employ molecular sieves of 3, 4, and 5 Å pore diameters for effective dryness and removal of residual amounts of water from ionic liquids. Here, 1-methyl-1-propylpiperidinium bis(trifluoromethylsulfonyl)imide (MPPip-TFSI) and 1-butyl-1-methylpyrrolidinium bis(trifluoromethylsulfonyl)imide (BMP-TFSI) (Scheme 1) are used as reprehensive examples for hydrophobic ionic liquids with different cations. Notably, 3 Å and 4 Å molecular sieves can effectively reduce the amount of residual water to $< 1\ mg \cdot L^{-1}$. Interestingly, a significant change in the electrochemical behavior of Au(111) after drying those ionic liquids indicates that the presence of even traces of water influence the physical and electrochemical properties of ionic liquids. Additionally, the influence of this water on the electrochemical Mg deposition/dissolution was studied in MPPip-TFSI/tetraglyme (1 : 1) + 100 mM $Mg(TFSI)_2$ + 10 mM $Mg(BH_4)_2$. Interestingly, the results of Mg deposition/dissolution in dried MPPip/tetraglyme system compared to that of the as-received system reveals: i) a higher stability of Mg as well as Ag/AgCl as reference electrodes, ii) a lower solution resistance, and iii) a higher double layer capacitance by a factor of 2.

Results and Discussion

In this study, we have investigated the effect of molecular sieves of different pore sizes (3 Å, 4 Å, and 5 Å) on the water concentration in ionic liquids. Notably, ionic liquids of different polarities exhibit distinctly different degrees of interaction with water. Still, the tendency of water adsorption and miscibility in ionic liquids is connected to the anion counterpart.[43] Therefore, we have selected two hydrophobic ionic liquids with different cations characters; MPPip-TFSI and BMP-TFSI. Despite both ionic

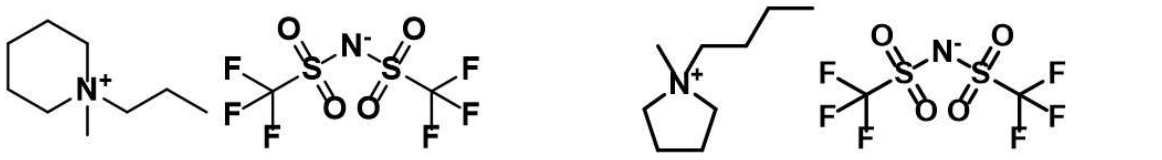

1-Methy 1-propylpiperidinium bis(trifluormethylsulfonyl)imide 1-Butyl 1-methylpyrrolidinium bis(trifluormethylsulfonyl)imide

Scheme 1. Chemical structure of MPPip-TFSI (left) and BMP-TFSI (right).

liquids bearing the same anionic part (TFSI), the MPPip-TFSI is more hydrophobic than BMP-TFSI due to its different cation.[44]

Water content

Figure 1 compares the water content of as-received MPPip-TFSI and BMP-TFSI and after the heat and vacuum treatment in the presence and absence of molecular sieves of different pore sizes. The as-received MPPip-TFSI and BMP-TFSI have a relatively high water concentration of 91 and 65 mg·L^{-1}, respectively. Interestingly, the water content decreases tremendously (to $<$1 mg·L^{-1}) upon treatment of both ionic liquids with the 3 or 4 Å molecular sieves. In contrast, using 5 Å molecular sieves results in about 10-fold higher water concentration (~ 10 mg·L^{-1}). Still, this water concentration is lower than that observed after heat and vacuum treatment only, which exhibits 15 mg $^{-1}$ and 30 mg $^{-1}$ for MPPip-TFSI and BMP-TFSI, respectively. These observations indicate that molecular sieves can indeed further decrease water from ionic liquids even at trace levels. However, the pore size of the molecular sieve is crucial for effectively removing water and, consequently, obtaining (almost) water-free ionic liquids. The adsorption process of water molecules on the molecular sieves occurs via three stages related to different adsorption sites in the crystals.[40] The efficiency of the molecular sieves to adsorb water is strongly influenced by their framework structure which contains channels and voids occupied by water molecules and different cations. The molecular sieves lose their water molecules and become dehydrated upon thermal activation. Thus, new adsorption sites will be available for the adsorption of water or other species which possess a comparable size to the accessible pores.[45] The water molecule diameter is about 2.8 Å, which is closer to 3 Å and 4 Å, whereas 5 Å molecular sieves are apparently too large.[46] Therefore, 3 Å and 4 Å molecular could have been expected to be efficient for water removal. Furthermore, neither the cationic nor anionic counterparts of the investigated ionic liquids can be adsorbed on molecular sieves due to their large sizes.[47]

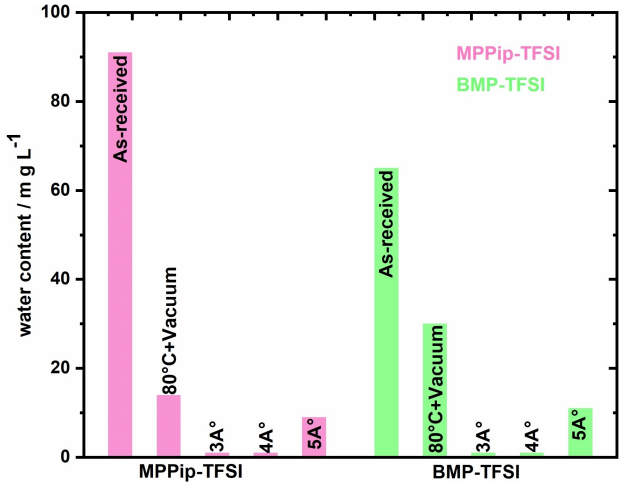

Figure 1. Water content of the MPPip-TFSI and BMP-TFSI as received, after the heat and vacuum treatment in the presence and absence of molecular sieves with different pores.

Spectroscopic and analytical investigations

NMR spectroscopy, FTIR spectroscopy, and electrospray ionized mass spectroscopy (ESI-MS) were employed to study the influence of 3 Å and 4 Å molecular sieves on the structural stability of MPPip-TFSI and BMP-TFSI upon treatment (Figures S1–S3 in the Supporting Information). Remarkably, there are no chemical shifts in the ^{1}H, ^{13}C, and ^{19}F spectra of the MPPip-TFSI and BMP-TFSI after treatment with 3 Å or 4 Å molecular sieves compared to their original spectra, as illustrated in Figure S1. Furthermore, the FTIR spectra show that the treatment does also not affect their stretching and bending vibrations (Figure S2). Figure S3 shows the ESI-MS mass spectra for the MPPip-TFSI and BMP-TFSI before and after treatment with 3 Å and 4 Å molecular sieves, revealing no influence on their molecular weights, which indicates a similar chemical structure after treatment. These findings reveal that 3 Å and 4 Å molecular sieves significantly reduce the water content of both ionic liquids without affecting their structural stability and integrity. In other words, the cations and anions of both ionic liquids are still held together without any observed structural decomposition upon removing water molecules from the system.

Electrochemical characterization

Cyclic voltammetry is a straightforward and sensitive technique commonly used to investigate the electrochemical behavior of ionic liquids. Furthermore, highly-stable and well-defined metal surfaces are typically employed for such fundamental studies.[48] Therefore, the electrochemical behavior of an Au(111) electrode in MPPip-TFSI and BMP-TFSI was studied. Ionic liquids are stable within a rather broad potential window, where the regular potential regimes of MPPip-TFSI and BMP-TFSI are −3.27 to 2.23 V *vs.* Ag/AgCl[49] and −3.01 V to 2.71 V *vs.* Ag/AgCl,[50] respectively. Additionally, the oxidation of Au(111) in MPPip-TFSI and BMP-TFSI has been observed at potentials $>$2.23 V and $>$2.71 V *vs.* Ag/AgCl, respectively.[49,50] The presence of water, even at low concentrations, might trigger cathodic corrosion of Au(111) at potentials negative to the hydrogen evolution regime and consequently induces prominent structural changes.[37,51] Thus, we have investigated the electrochemical behavior of Au(111) in MPPip-TFSI and BMP-TFSI at potential regimes, where both the electrolyte and working electrode are stable.

Figures 2 and 3 display the electrochemical behavior of MPPip-TFSI and BMP-TFSI on Au(111) at 5 mV·s^{-1} before and after treatment with 3 Å, 4 Å, or 5 Å molecular sieves. As shown in Figure 2a, the cyclic voltammogram (CV) of the as-received MPPip-TFSI demonstrates two cathodic peaks at approximately −0.70 V and −1.15 V *vs.* Ag/AgCl that are assigned to either the adsorption and restructuring of MPPip^{+}[54,55] and/or the reduc-

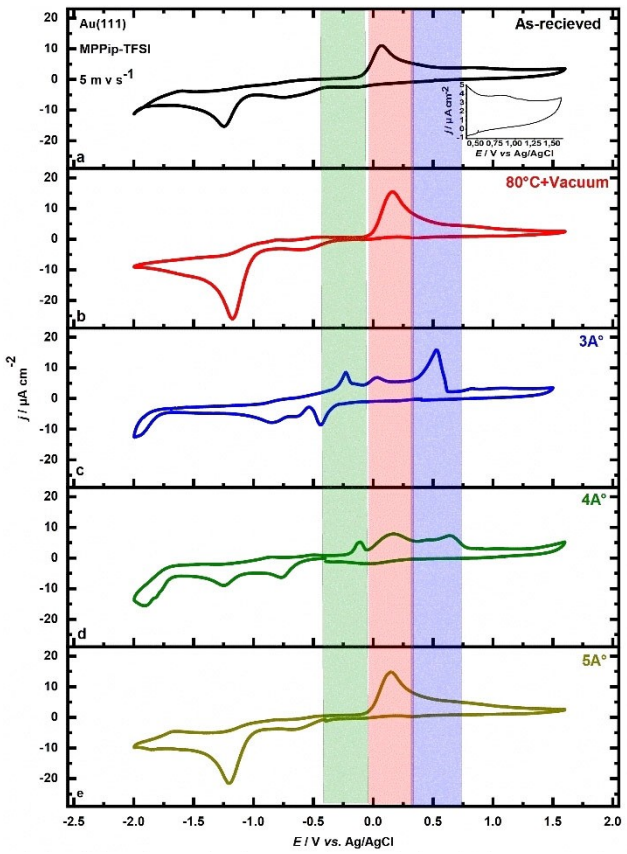

Figure 2. Cyclic voltammograms of the electrochemical behavior of MPPip-TFSI a) as-received, b) treated with vacuum + 80 °C, c) treated with 3 Å molecular sieves, d) treated with 4 Å molecular sieves, and e) treated with 5 Å molecular sieves on Au(111) with scan rate 5 mV·s^{-1} vs. Ag/AgCl. The blue column resembles a new peak at approximately 0.80 V vs. Ag/AgCl, the red column resembles the main anodic peak at 0.20 V vs. Ag/AgCl and the green column resembles a new anodic peak at approximately −0.21 V vs. Ag/AgCl.

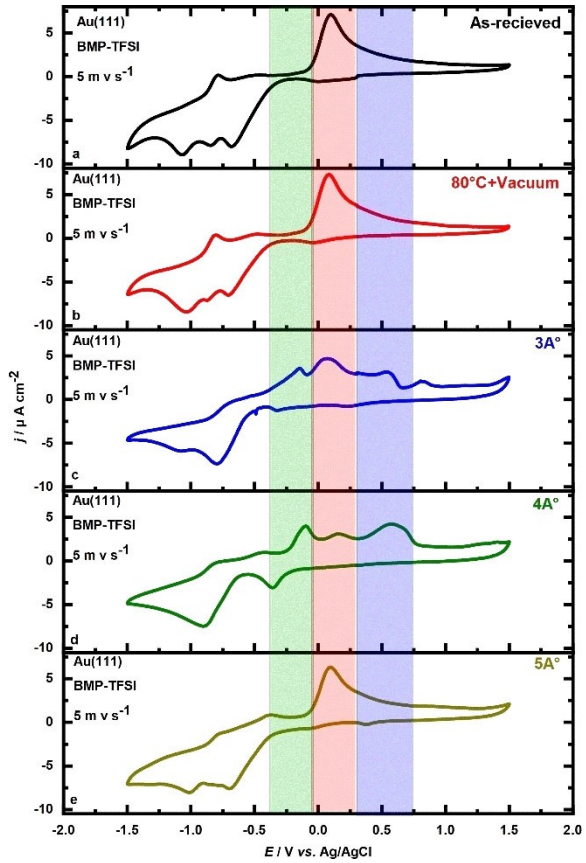

Figure 3. Cyclic voltammograms of the electrochemical behavior of BMP-TFSI a) as-received, b) treated with vacuum + 80 °C, c) treated with 3 Å molecular sieves, d) treated with 4 Å molecular sieves, and e) treated with 5 Å molecular sieves on Au(111) with scan rate 5 mV·s^{-1} vs. Ag/AgCl. The blue column resembles a new peak at approximately 0.80 V vs. Ag/AgCl, the red column resembles the main anodic peak at 0.20 V vs. Ag/AgCl and the green column resembles a new anodic peak at approximately −0.21 V vs. Ag/AgCl.

tion of $TFSI^-$[52,53] on Au(111). Moreover, the anodic peaks at around 0.20 V and 0.80 V *vs.* Ag/AgCl (inset Figure 2a) are attributed to the oxidation of the cathodic products either $MPPip^+$ or $TFSI^-$.[55] The cyclic voltammogram of the as-received BMP-TFSI exhibits three cathodic peaks at approximately −0.70 V, −0.85 V, and −1.10 V *vs.* Ag/AgCl that can be assigned to either the adsorption and restructuring of BMP^+[54,55] and/or the reduction of the $TFSI^-$.[52,53] The anodic peak at around 0.20 V *vs.* Ag/AgCl is attributed to the oxidation of the cathodic products of either BMP^+ or $TFSI^-$.[55] According to previous studies, STM reveals that the adsorption of BMP-TFSI on Au(111) has two different structures; short-range order and long-range order. Additionally, the BMP-TFSI adsorbates form islands due to the strong interactions between the adsorbed species.[56]

The treatment with heat and vacuum and in the presence of 5 Å molecular sieves hardly influenced the electrochemical behavior of MPPip-TFSI and BMP-TFSI (Figure 2b, e and Figure 3b and e). Interestingly, new anodic features arise upon the treatment with heat and vacuum in the presence of 3 Å and 4 Å molecular sieves for MPPip-TFSI and BMP-TFSI, as shown in Figure 2c–d and Figure 3c–d, respectively assigned with three colored columns. Upon lowering the water content (< 1 mg·L^{-1}), the main anodic peak at around 0.20 V *vs.* Ag/AgCl is significantly decreased in MPPip-TFSI as well as in BMP-TFSI (red column), while the peak at approximately 0.80 V *vs.* Ag/AgCl in MPPip-TFSI becomes more pronounced (blue column). Additionally, a new anodic peak at approximately −0.21 V *vs.* Ag/AgCl is observed in both ionic liquids (green column). The charge density of the cathodic peak of MPPip-TFSI at roughly −1.15 V *vs.* Ag/AgCl is substantially reduced. Such findings reveal that the presence of water (even at trace levels) considerably affects the electrochemical behavior of the ionic liquid and electrode surface.

Previously, the purification of 1-butyl-3-methylimidazolium hexafluorophosphate (BMIM-PF_6) upon treatment with similar molecular sieves was investigated.[33] It was observed that the electrochemical behavior of Au(111) in the hydrophilic BMIM-PF_6 turned out to be different after treatment with 3 Å, 4 Å, and 5 Å molecular sieves compared to the treatment with only heat at 80 °C and vacuum. In the case of using 3 Å molecular sieves, the cathodic peaks at −0.2 V *vs.* Ag/AgCl were still observed and the corresponding anodic feature became flattened.

Furthermore, the cathodic peak at −0.75 V *vs.* Ag/AgCl was enhanced. On the other hand, the treatment of BMIM-PF_6 with 4 Å and 5 Å molecular sieves caused the appearance of additional anodic and cathodic peaks. These changes were correlated to the impurities introduced into the system by using 4 Å and 5 Å molecular sieves. However, the information about the chemical stability and water content of BMIM-PF_6 upon treatment with molecular sieves was not mentioned in this study.[33] Nevertheless, in our present work, the molecular sieves were washed with pure water before their activation to remove any dirt and contaminants. Furthermore, we were able to prove that the molecular sieves do not introduce any impurities to the system, and the chemical stability of both studied ionic liquids is maintained after treatment with molecular sieves. Additionally, the difference in the electrochemical behavior in our study compared to Gnahm's study could be due to the handling and drying of the ionic liquid.

It is known that the existence of water molecules in the double layer disrupts the interactions between anions and cations due to the formation of strong hydrogen bonds with the amino and the sulfonic groups. The hydrogen bonds induce a reorientation of the ions, leading to changes in the anion-cation super-structure.[21] Furthermore, the presence of water inside the ionic liquid has an influence on the hydrogen bonding as well as the depolarization effects.[57] The newly observed peaks in the cyclic voltammograms of MPPip-TFSI and BMP-TFSI upon lowering the water content ($< 1\ mg \cdot L^{-1}$) might be due to the formation of different anion-cation structures induced by minimizing the influence of hydrogen bonds and the electrosorption of water molecules. Moreover, lowering the water content reduces the columbic interactions among ions and between ions and the electrode surface.[58]

To investigate whether cation exchange occurs between the ionic liquids and molecular sieves that might be responsible for the appearance of these new CV-peaks, we compared the cyclic voltammogram of the as-received MPPip-TFSI with the system after the addition of 5 mM NaTFSI (Figure S4). The addition of Na^+ ions did not show the same anodic peaks that appear after molecular sieving of MPPip-TFSI. Therefore, we expect that such changes are indeed connected to lowering the water content inside the ionic liquid.

Electrochemical impedance spectroscopy

As proven by cyclic voltammetry, the presence of residual amounts of water in ionic liquids has a significant impact on their electrochemical behavior. Thus, further investigations are required to study the effect of water on the double-layer capacitance and the electrode/electrolyte interface. For many years, ionic liquids have been intensively studied in our institute to investigate their electrochemical behavior and the electrode/electrolyte interfaces by electrochemical and surface-sensitive techniques,[33,53,59–65] in particular the electrochemistry of dried MPPip-TFSI on Au(100).[66] As a continuation of this work, here we further investigated the effect of a trace amount of water in ionic liquids on the electrochemical performance and double-layer capacitance (C_{dl}) using electrochemical impedance spectroscopy (EIS) at the open circuit potential (OCP). Figure 4 shows the Nyquist plots of as-received vs. dried MPPip-TFSI and

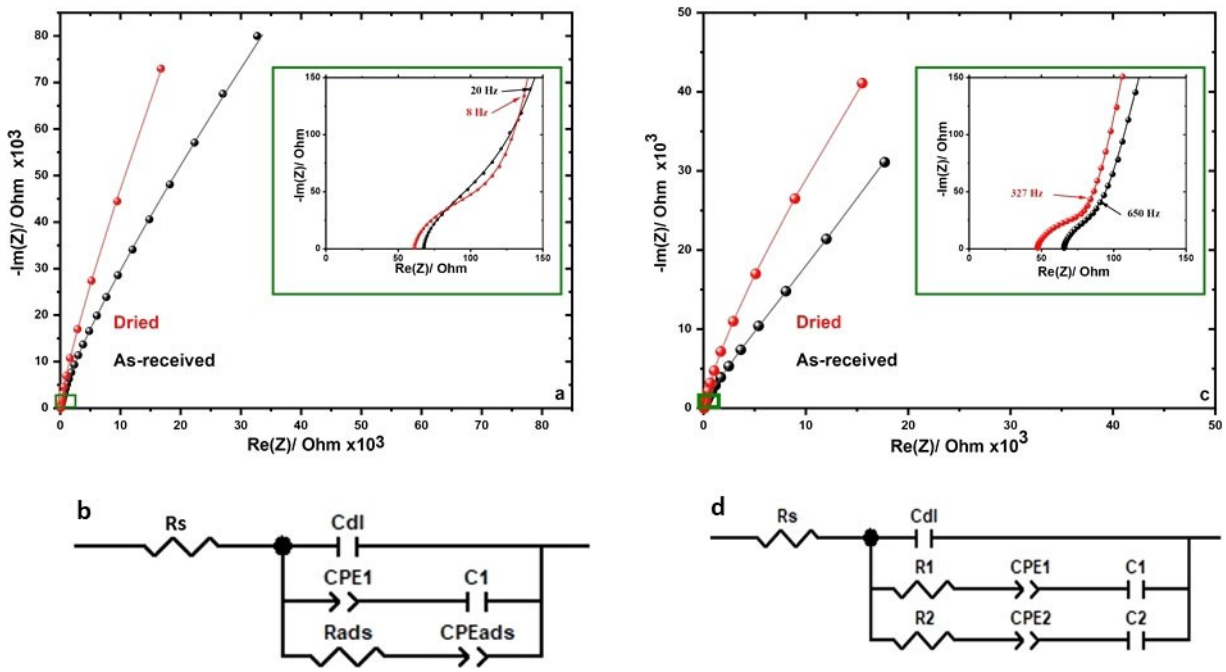

Figure 4. a) Nyquist plots for as-received and dried MPPip-TFSI with 4 Å molecular sieves on Au(111) electrode (inset shows a zoom-in at the high-frequency region, b) equivalent circuit used to fit the results of MPPip-TFSI, c) Nyquist plots for as-received and dried BMP-TFSI with 4 Å molecular sieves on Au(111) electrode (inset shows a zoom-in at the high-frequency region and d) equivalent circuit used to fit the results of BMP-TFSI. The black and red balls in a) and c) represent the experimentally obtained data, while the lines represent the fit results.

BMP-TFSI with 4 Å molecular sieves, showing an incomplete semicircle at the high-frequency region and a spike at the low-frequency region. The dried ionic liquids showed a slightly lower solution resistance than the as-received ones, which is due to the interaction of water molecules with ionic liquid ions, resulting in a slower diffusion and consequently lower conductivity (higher solution resistance). In the case of MPPip-TFSI, the slope of the low-frequency spike is higher for the dried ionic liquid than for the as-received, which indicates the enhanced capacitive-like behavior and less electrode surface perturbation by adsorption processes, which are more dominant in the presence of a residual amount of water. Based on previous studies,[53,62,65,67] it can be concluded that simple equivalent circuits are not adequate to fit the double layer and ionic liquid/electrode interfaces. However, the EIS spectra of both as-received and dried MPPip-TFSI can be very well fitted (typically with $\chi^2 \approx 10^{-5}$) by the equivalent circuit shown in Figure 4b, consisting of a solution resistance in series with a parallel combination of three capacitive branches that describe the double-layer capacitance and surface processes such as adsorption and double-layer rearrangement occurring at the electrode/electrolyte interface. The values of the fitting parameters are tabulated in Table 1. As clearly shown, the presence of water residues affects both C_{dl} and the adsorption of ions on the electrode surface. The dried MPPip-TFSI showed a relatively high double layer capacitance of 1.73 $\mu F \cdot cm^{-2}$ compared to 1.37 $\mu F \cdot cm^{-2}$ for the as-received that is attributed to the interaction of water molecules with the ionic liquid ions that leads to an increase in the double layer thickness and consequently decreases the value of C_{dl}.

The most interesting branches of the equivalent circuit are branches 2 and 3 which describe the surface perturbation processes such as the adsorption of ions on the electrode surface, being responsible for changes on the electrode surface. The capacitive values in the second branch are closely related to the interfacial capacitance, the greater their values, the slower are surface perturbations. As shown in Table 1, the dried MPPip-TFSI has nearly double the values of the constant phase element CPE_1 and the capacitance C_1 (second branch) which means the surface perturbation is much slower in the dried ionic liquids than in the presence of residual water contents that mainly facilities surface perturbations. Moreover, the presence of water traces minimize the adsorption resistance, allowing for more surface changes when an electric potential is applied, such as in corrosion processes and surface reconstructions, compared to the dried ionic liquids.[53,63] Additionally, this increased adsorption affinity in the presence of water molecules may also block some of the active sites on the electrode surface. All of the previous observations explain the disappearance of some redox peaks in the cyclic voltammogram of as-received MPPip-TFSI shown in Figure 2. In contrast to MPPip-TFSI, as-received BMP-TFSI showed less imaginary impedance than the dried BMP-TFSI as well as the equivalent circuit used to get an adequate fitting is different as shown in Figure 4d. The fitting parameters showed a huge change in the interfacial resistances and capacitances upon BMP-TFSI drying (R_2 and C_2). A lower resistance and a greater capacitance were obtained after 4 Å molecular sieving and drying of BMP-TFSI, indicating the great effect of the presence of water residues on the ionic liquid/electrode interface. On the other hand, there are no significant differences in the C_{dl} values between as-received and dried BMP-TFSI ionic liquids. As both MPPip-TFSI and BMP-TFSI share the same anions, this different behavior could be associated with the change in the cation size and the degree of hydrophobicity. The BMP^+ cation is less hydrophobic than $MPPip^+$, suggesting more water interaction with BMP^+ compared to $MPPip^+$,[44] which is also observed in the CVs of both ionic liquids. The cyclic voltammograms of BMP-TFSI showed some differences in the water-cation interactions compared to MPPip-TFSI, which is indicated by the appearance of well-resolved peaks in the cathodic direction for as-received BMP-TFSI compared to the dried one. Moreover, EIS fitting parameters shown in Table 1 revealed a higher adsorption resistance in the case of MPPip-TFSI (R_{ads}) than BMP-TFSI, indicating that stronger ion adsorption occurs on the surface of Au(111) in the case of BMP-TFSI (R_1). Herein, one can conclude that the ionic liquid cation has a significant impact on the electrochemical

Table 1. Fitting parameters extracted from fitting the EIS results of MPPip-TFSI and BMP-TFSI by using equivalent circuits shown in Figures 4 b and d, respectively.[a]

Property	MPPip-TFSI as-received	dried	Property	BMP-TFSI as-received	dried
R_s [Ω]	67.46	61.18	R_s [Ω]	65.67	47.4
C_{dl} [μF cm^{-2}]	1.37	1.73	C_{dl} [μF cm^{-2}]	2.06	1.9
CPE_1 [mS s^n]	1.2	2.8	R_1 [Ω]	28.38	36.9
n_1	0.2547	0.1806	CPE_1 [mS s^n]	1.4	1.5
C_1 [μF cm^{-2}]	7.13	12.97	n_1	0.3804	0.4231
R_{ads} [kΩ]	12.9	29.2	C_1 [μF cm^{-2}]	7.8	15.5
CPE_2 [μS s^n]	9.6	7.05	R_2 [Ω]	1386	18.86
n_2	0.6023	0.6525	CPE_2 [μS s^n]	33.8	17.4
			n_2	0.5387	0.5751
			C_2 [mF cm^{-2}]	2.4	9.1
uncertainty	0.0056	0.0048	uncertainty	0.0019	0.0062
χ^2	4.9×10^{-5}	5.2×10^{-5}	χ^2	2.1×10^{-5}	6.9×10^{-5}

[a] R_s are the solution resistances, C_{dl} are the double layer capacitances, CPE are the constant phase elements, R and C are additional resistances and capacitances, and χ^2 is a measure for the quality of the fit.

properties. Therefore, future studies will aim at connecting the impedance spectra with corresponding *in-situ* surface studies.

Probing the effect of water through Mg deposition/dissolution

The passivation of the working electrode is one of the main challenges when working with ionic liquids due to the presence of small water traces. Therefore, a well-known established system of ionic liquids with tetraglyme was used to test the effect of water on magnesium deposition/dissolution.[32] Despite the common use of magnesium borohydride $Mg(BH_4)_2$ as a water scavenger,[32,35,68–70] in this study, we show that the dryness of the electrolyte is a critical aspect even in the presence of $Mg(BH_4)_2$. In our study, we focused on two electrolyte systems: the as-received one and after drying with 4 Å molecular sieves. The water content for the investigated as-received system is 91 $mg \cdot L^{-1}$ for MPPip-TFSI and 262 $mg \cdot L^{-1}$ for tetraglyme and the dried system is <1 $mg \cdot L^{-1}$ for MPPip-TFSI and 17 $mg \cdot L^{-1}$ for tetraglyme. A Pt-foil (diameter = 12 mm) was used as both working and counter electrodes and a Mg or Ag/AgCl wire was used as a pseudo-reference to monitor the influence of water (in the $mg \cdot L^{-1}$ range) on Mg deposition/dissolution and the stability of the reference electrodes. Figure 5a shows the corresponding cyclic voltammograms of Mg deposition and dissolution from MPPip-TFSI/tetraglyme (1:1) with 100 mM $Mg(TFSI)_2$ and 10 mM $Mg(BH_4)_2$ before and after treatment with the 4 Å molecular sieve. A significant potential shift for about 0.9 V *vs.* Mg/Mg^{2+} was observed with the as-received system when using the Mg wire as reference electrode, which corresponds to a pronounced influence of water in passivating the reference electrode and causing a notable potential difference, being in agreement with the observation in reported Reference.[71] So, a more stable Ag/AgCl reference electrode was used for the measurement as shown in Figure 5b. In the cyclic voltammogram of the dried MPPip-TFSI/tetraglyme (1:1) system, the Mg deposition occurs at −2.7 V *vs.* Ag/AgCl, while dissolution occurs at around −2 V *vs.* Ag/AgCl. In comparison, the as-received MPPip-TFSI/tetraglyme (1:1) system shows Mg deposition at −3 V and dissolution at −2.3 V *vs.* Ag/AgCl, thus being shifted by around 0.3 V compared to the dried system. That change in the potential is due to the higher water content inside the as-received system, which also causes a decrease in the current density compared to the dried system.

EIS measurements of both as-received and dried MPPip-TFSI containing tetraglyme, 100 mM $Mg(TFSI)_2$, and 10 mM $Mg(BH_4)_2$ on polycrystalline Pt electrode showed an arc at the high-frequency region (mainly higher than 10 Hz) and a spike at the low-frequency region. Similar to the results in pure ionic liquids, the as-received ionic liquid-containing electrolyte revealed higher solution resistance and higher impedance at the low-frequency region as shown in Figure 6. To get more insights into the interface, an equivalent circuit shown in the inset of Figure 6 was used to fit the EIS curves and the fitting results are tabulated in Table S1. The equivalent circuit used to fit the results is closer to circuits used to fit pure ionic liquids with little modifications due to the presence of magnesium salts and tetraglyme in the system as well as the differences between polycrystalline Pt and single crystalline Au(111). In this case, and besides the solution resistance, the high-frequency region is described by the double layer capacitance, C_{dl}, which is independent of the type of metal electrode and more likely dependent on the nature of the ionic liquid, especially the cations seem to be dominating here.[53,72] It is found that the value of C_{dl} decreases in the presence of water as shown in Table S1. The as-received electrolyte showed nearly half the C_{dl} value compared to the dried electrolyte, 2.5 $\mu F \cdot cm^{-2}$ and 5 $\mu F \cdot cm^{-2}$, respectively. This means that the presence of water molecules leads to a thicker double-layer region and consequently, a smaller capacitance value. The significant effect of water residues on C_{dl} in this case compared to the pure ionic liquids is attributed to the extra water residues added by the Mg salts and the tetraglyme solvent. This finding is also

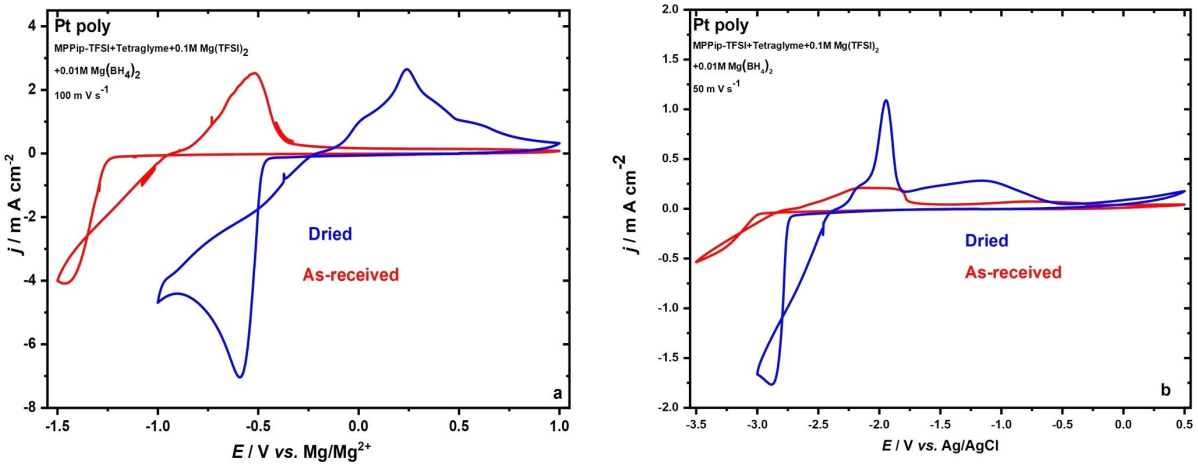

Figure 5. CVs showing the magnesium deposition and dissolution using MPPip-TFSI/tetraglyme (1:1) dried with 4 Å molecular sieves and as-received ionic liquid with tetraglyme, 100 mM $Mg(TFSI)_2$ and 10 mM $Mg(BH_4)_2$ at a scan rate of 100 $mV \cdot s^{-1}$ using a Mg reference electrode (left) and at a scan rate of 50 $mV \cdot s^{-1}$ using a Ag/AgCl reference electrode (right).

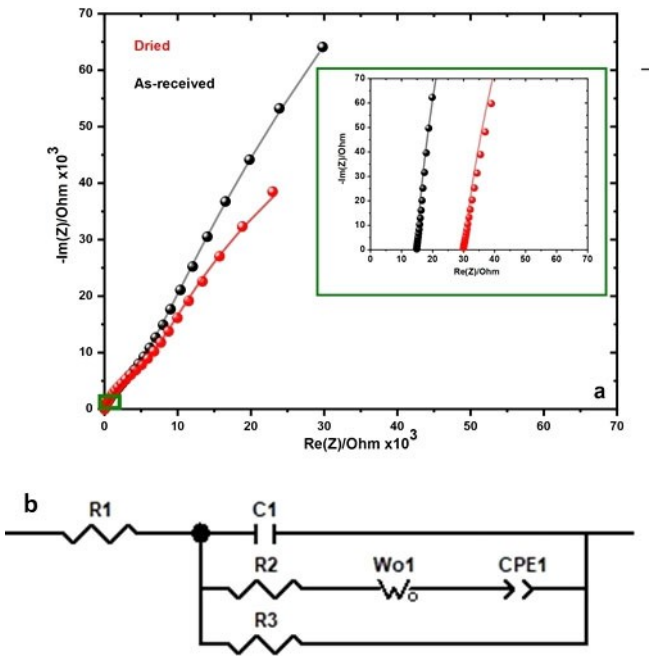

Figure 6. Top: Nyquist plot for MPPip-TFSI/tetraglyme (1 : 1) dried with 4 Å molecular sieves and as-received with 100 mM $Mg(TFSI)_2$ and 10 mM $Mg(BH_4)_2$ on Pt electrode where the black and red balls represent the experimentally obtained data while the lines represent the fit results (inset: zoom-in of the high-frequency region); Bottom: the equivalent circuit used to fit the results.

consistent with the previously mentioned assumption that water molecules interact strongly with the ions in the system, affecting the solvation behavior and orientation of ionic liquids, and consequently disrupting the interface.

The second branch in the equivalent circuit mainly describes the pseudocapacitive processes which are most likely related to the adsorption processes that could happen on the electrode surface. It consists of the adsorption resistance, R_{ads} (R_2), in series with an open Warburg element and a constant phase element, CPE_{ads}. It is worth mentioning that all attempts to replace the CPE with pure capacitances were not successful in obtaining an adequate fitting as shown in Figures S5–S7 and Tables S2 and S3. However, interpretation in terms of an adsorption capacitance is complicated by the dimensionality of the CPE's impedance:

$$Z_{CPE} = \frac{1}{Q \times (j\omega^a)} \quad (1)$$

Only when $a = 1$, the CPE behaves as a pure capacitor, while for $a = 0.5$ it acts as a Warburg element indicating diffusion-limited kinetics. In both cases, the CPE exponent is between 0.61 to 0.66, which makes the calculation of the capacitive values of adsorption difficult. Therefore, in both cases, we cannot explicitly comment on the value of adsorption capacitance.

The third branch in the equivalent circuit consists only of a pure resistance that can be assigned to the charge transfer resistance, R_{ct}, due to the presence of magnesium salts. This branch should be omitted in case of pure MPPip-TFSI on polycrystalline or single crystalline Pt electrodes and consists of a serial *R*–CPE–*C* circuit, or a subset of it (CPE, *R*–*W*–*C*, etc.) for single crystalline Au(100) or Ag(100).[66] As shown in Table S1, the value of R_{ct} decreases upon further drying the electrolyte compared to the as-received, which explains the smaller onset potential of Mg deposition in the dried system compared to the as-received. We have also tried to fit the results with different capacitance methods by changing some of the components, which did not affect much the value of the C_{dl} but affected the quality of fitting as clearly shown in the supporting information, Table S2. Additionally, all attempts to omit the third branch or modify it were not successful in producing adequate fittings. All of these findings show the importance of the drying of the ionic liquids for obtaining reproducible and reliable measurements, which is also in agreement with other previous reports.[33,73] In closing, we have to mention that the preparation of the surface of the working electrode is also essential for electrochemical investigations as the surface roughness and adsorbed species may strongly influence the EIS behavior.

Conclusions

We have studied the influence of trace amounts of water on the electrochemical performance of ionic liquids. 3 Å and 4 Å molecular sieves have successfully removed these trace amounts of water for ionic liquids compared to 5 Å molecular sieves, showing water contents of $< 1\ mg \cdot L^{-1}$ by Karl–Fischer titration. The electrochemical behavior of Au(111) in two hydrophobic ionic liquids having different cations, *i.e.*, MPPip-TFSI and BMP-TFSI, was studied. After drying with 3 Å and 4 Å molecular sieves, new anodic features arise in both ionic liquids, affirming the influence of trace amounts of water on the electrochemical behavior. Furthermore, the electrochemical impedance showed that the dried ionic liquids had a slightly lower solution resistance compared to the as-received. Moreover, the dried MPPip-TFSI with 4 Å molecular sieves showed a relatively higher double-layer capacitance of $1.73\ \mu F \cdot cm^{-2}$ compared to $1.37\ \mu F \cdot cm^{-2}$ for the as-received. Likewise, the dried BMP-TFSI with 4 Å molecular sieves demonstrated lower resistance and larger capacitance compared to the as-received electrolyte. NMR, ESI-MS, and FTIR confirmed the chemical stability of both ionic liquids after treatment with molecular sieves. Additionally, cyclic voltammetry and electrochemical impedance spectroscopy for as-received Mg-containing electrolytes showed that the drying step seems to be crucial for achieving a stable Mg deposition/dissolution behavior. In the as-received system, a potential shift of 0.9 V *vs.* Mg/Mg^{2+} indicates the passivation of Mg as an anode in the presence of residual water contents. The as-received ionic liquid-containing electrolyte revealed a higher solution resistance and higher impedance at the low-frequency region as well as nearly half the value of C_{dl} compared to the dried one. The electrode surface perturbation as well as properties are very much influenced by the presence of even trace amounts of water. Therefore, drying ionic liquids is a crucial step for studying the

electrochemical performance or using them as electrolytes in metal ion batteries.

Experimental Section

Chemicals

1-Methyl-1-propylpiperidinium bis(trifluoromethylsulfonyl)imide (MPPip-TFSI) was purchased from Iolitec with >99% purity (water $<100\ mg\cdot L^{-1}$ and halides $<100\ mg\cdot L^{-1}$). 1-Butyl-1-methylpyrrolidinium bis(trifluoromethylsulfonyl)imide (BMP-TFSI, >98.5%) and molecular sieves with three different pore diameters (3, 4, and 5 Å) were purchased from Merck. Magnesium(II) bis(trifluoromethanesulfonyl)imide ($Mg(TFSI)_2$,99.5%) was obtained from Solvionic. Additionally, tetraglyme (≥99%) and magnesium borohydride ($Mg(BH_4)_2$, 95%) were bought from Sigma Aldrich.

Electrolyte preparation

Molecular sieves were washed with ultra-pure water (18.2 MΩ cm, $TOC \leq 3\ \mu g\cdot L^{-1}$) several times before drying at 80 °C in the drying oven for 12 h. For the activation of the molecular sieves, they were heated at 300 °C for 5 h in a vacuum oven. The vacuum oven is placed inside a MBRAUN LABStar glovebox flooded with N_2 (5.0, MTI IndustrieGase AG) or atmosphere (O_2, $H_2O \leq 0.5\cdot mg\,L^{-1}$). For drying the ionic liquid, molecular sieves were added with a ratio of around 1.3 g of molecular sieves to 3 ml of ionic liquid and then heated at 80 °C under low pressures (10^{-3} mbar) for 20 h. Afterwards, the treated ionic liquids were stored inside the glovebox for experimental investigations. Tetraglyme was stored over 4 Å molecular sieves for a week inside the glovebox. In order to obtain the electrolyte for Mg deposition, $Mg(TFSI)_2$ (dried under vacuum at 80 °C for 16 h) and $Mg(BH_4)_2$ (without drying) were dissolved in a mixture of MPPip-TFSI and tetraglyme with a ratio of 1:1 at 60 °C inside the glovebox for 2 h.

Structural characterization

^1H, ^{13}C, and ^{19}F NMR spectra were recorded using a 400 MHz NMR from Bruker. The ionic liquids were dissolved in dimethyl sulfoxide (DMSO) before recording. Afterwards, the spectra were analyzed with the MNOVA software. The mass spectra (ESI-MS) were recorded by using Bruker SolariX MS and before performing the recordings the ionic liquids were dissolved in isopropanol. Attenuated total reflection Fourier transform infrared (ATR-FTIR) spectra were recorded using a Thermo-Scientific Nicolet 6700 FTIR in the range from 550 to 3500 cm^{-1}. The electrochemical measurements were performed using a Zahner IM6 potentiostat installed inside the glove box. The water content of all samples has been determined by Karl–Fischer titration (Metrohm GmbH & Co.) installed inside the glove box.

Electrochemical characterization

Cyclic voltammetry and electrochemical impedance spectroscopy measurements were performed in homemade cells of KelF with a small volume capacity (0.25 cm^3).[33] An Au(111) single crystal (MaTeck GmbH) with 12 mm in diameter was used as a working electrode and a platinum wire (MaTeck GmbH >99%) was used as a counter electrode. A quasi-reference electrode of Ag/AgCl was used. The silver wire (MaTeck GmbH >99%) was immersed in 0.1 M HCl and $10\ mA\cdot cm^{-2}$ was passed for 1 min to coat the silver wire with a chloride layer. Before performing the electrochemical measurement, the Au(111) electrode was annealed in a muffle furnace (Carbolite CWF 1200) for 2 h at 960 °C. The electrochemical impedance spectra were recorded with an amplitude of 5 mV and a frequency range between 100 kHz and 100 mHz and ZView software was used to fit the results based on the complex non-linear least square method with the number of iterations equals 100.

Mg deposition/ dissolution

Cyclic voltammetry and electrochemical impedance spectroscopy measurements were performed in a three-electrode BOLA cell similar to the Swagelok cell using a Pt sheet (MaTeck GmbH, 99.9%) with 12 mm in diameter and 0.025 mm thickness as working and counter electrode, respectively, using a Biologic potentiostat. As reference electrodes, we used either a magnesium or an Ag/AgCl wire. Two glass fibre separators (Whatman GF/B) were soaked with 140 µl of MPPip-TFSI/tetraglyme (1:1) with 100 mM $Mg(TFSI)_2$ and 10 mM $Mg(BH_4)_2$ and one placed between the counter and reference electrodes and the other between the working and reference electrodes. The electrochemical impedance spectra were recorded with an amplitude of 10 mV in a frequency range from 100 kHz to 100 mHz.

Acknowledgements

This research was conducted as part of the German Research Foundation (DFG) under Project ID 390874152 (POLiS Cluster of Excellence) as well as the Schwerpunktprogramm (priority program) SPP-2248 "Polymer-based Batteries" under Project ID 441209207. Further, support by the state of Baden-Württemberg and the DFG through grant no. INST 40/574-1 FUGG as well as by the BMBF through the InnoSüd-project (Grant Agreement: 03IHS024D) is gratefully acknowledged. Open Access funding enabled and organized by Projekt DEAL.

Conflict of Interests

The authors declare no conflict of interest.

Data Availability Statement

The data that support the findings of this study are available from the corresponding author upon reasonable request.

Keywords: ionic liquids · molecular sieves · trace water · electrochemical impedance spectroscopy · Mg deposition

[1] Y. Zhan, W. Zhang, B. Lei, H. Liu, W. Li, *Front. Chem.* **2020**, *8*, 125.
[2] Q. Guo, W. Zeng, S.-L. Liu, Y.-Q. Li, J.-Y. Xu, J.-X. Wang, Y. Wang, *Rare Met.* **2021**, *40*, 290–308.
[3] D. S. Tchitchekova, D. Monti, P. Johansson, F. Bardé, A. Randon-Vitanova, M. R. Palacín, A. Ponrouch, *J. Electrochem. Soc.* **2017**, *164*, A1384–A1392.
[4] E. N. Keyzer, H. F. J. Glass, Z. Liu, P. M. Bayley, S. E. Dutton, C. P. Grey, D. S. Wright, *J. Am. Chem. Soc.* **2016**, *138*, 8682–8685.
[5] D. Aurbach, Z. Lu, A. Schechter, Y. Gofer, H. Gizbar, R. Turgeman, Y. Cohen, M. Moshkovich, E. Levi, *Nature* **2000**, *407*, 724–727.

[6] O. Tutusaus, R. Mohtadi, T. S. Arthur, F. Mizuno, E. G. Nelson, Y. V. Sevryugina, *Angew. Chem. Int. Ed.* **2015**, *54*, 7900–7904.
[7] R. Mohtadi, M. Matsui, T. S. Arthur, S.-J. Hwang, *Angew. Chem. Int. Ed.* **2012**, *51*, 9780–9783.
[8] K. A. See, K. W. Chapman, L. Zhu, K. M. Wiaderek, O. J. Borkiewicz, C. J. Barile, P. J. Chupas, A. A. Gewirth, *J. Am. Chem. Soc.* **2016**, *138*, 328–337.
[9] M. Salama, I. Shterenberg, H. Gizbar, N. N. Eliaz, M. Kosa, K. Keinan-Adamsky, M. Afri, L. J. W. Shimon, H. E. Gottlieb, D. T. Major, Y. Gofer, D. Aurbach, *J. Phys. Chem. C* **2016**, *120*, 19586–19594.
[10] I. Shterenberg, M. Salama, H. D. Yoo, Y. Gofer, J.-B. Park, Y.-K. Sun, D. Aurbach, *J. Electrochem. Soc.* **2015**, *162*, A7118–A7128.
[11] D. Aurbach, H. Gizbar, A. Schechter, O. Chusid, H. E. Gottlieb, Y. Gofer, I. Goldberg, *J. Electrochem. Soc.* **2002**, *149*, A115.
[12] Y. Gofer, R. Turgeman, H. Cohen, D. Aurbach, *Langmuir* **2003**, *19*, 2344–2348.
[13] R. Attias, M. Salama, B. Hirsch, Y. Goffer, D. Aurbach, *Joule* **2019**, *3*, 27–52.
[14] G. Yang, Y. Song, Q. Wang, L. Zhang, L. Deng, *Mater. Des.* **2020**, *190*, 108563.
[15] J. E. S. J. Reid, R. J. Gammons, J. M. Slattery, A. J. Walker, S. Shimizu, *J. Phys. Chem. B* **2017**, *121*, 599–609.
[16] C. D. Tran, S. H. De Paoli Lacerda, D. Oliveira, *Appl. Spectrosc.* **2003**, *57*, 152–157.
[17] L. Cammarata, S. G. Kazarian, P. A. Salter, T. Welton, *Phys. Chem. Chem. Phys.* **2001**, *3*, 5192–5200.
[18] R. M. Lynden-Bell, *Mol. Phys.* **2003**, *101*, 2625–2633.
[19] Y. Huang, Z. Wan, Z. Yang, Y. Ji, L. Li, D. Yang, M. Zhu, X. Chen, *J. Chem. Eng. Data* **2017**, *62*, 2340–2349.
[20] T. Kobayashi, J. E. S. J. Reid, S. Shimizu, M. Fyta, J. Smiatek, *Phys. Chem. Chem. Phys.* **2017**, *19*, 18924–18937.
[21] K. Wippermann, J. Giffin, S. Kuhri, W. Lehnert, C. Korte, *Phys. Chem. Chem. Phys.* **2017**, *19*, 24706–24723.
[22] J. E. S. J. Reid, A. J. Walker, S. Shimizu, *Phys. Chem. Chem. Phys.* **2015**, *17*, 14710–14718.
[23] N. Yaghini, J. Pitawala, A. Matic, A. Martinelli, *J. Phys. Chem. B* **2015**, *119*, 1611–1622.
[24] G. Feng, X. Jiang, R. Qiao, A. A. Kornyshev, *ACS Nano* **2014**, *8*, 11685–11694.
[25] U. Schröder, J. D. Wadhawan, R. G. Compton, F. Marken, P. A. Z. Suarez, C. S. Consorti, R. F. de Souza, J. Dupont, *New J. Chem.* **2000**, *24*, 1009–1015.
[26] Y. Zhong, J. Yan, M. Li, L. Chen, B. Mao, *ChemElectroChem* **2016**, *3*, 2221–2226.
[27] M. Xu, D. G. Ivey, Z. Xie, W. Qu, E. Dy, *Electrochim. Acta* **2013**, *97*, 289–295.
[28] Z. Ma, D. R. MacFarlane, M. Kar, *Batteries & Supercaps* **2019**, *2*, 115–127.
[29] G. Zhou, K. Jiang, Z. Wang, X. Liu, *Chin. J. Chem. Eng.* **2021**, *31*, 42–55.
[30] S. Randström, M. Montanino, G. B. Appetecchi, C. Lagergren, A. Moreno, S. Passerini, *Electrochim. Acta* **2008**, *53*, 6397–6401.
[31] B. K. Sweeny, D. G. Peters, *Electrochem. Commun.* **2001**, *3*, 712.
[32] Z. Ma, M. Forsyth, D. R. MacFarlane, M. Kar, *Green Energy & Environ.* **2019**, *4*, 146–153.
[33] M. Gnahm, D. M. Kolb, *J. Electroanal. Chem.* **2011**, *651*, 250–252.
[34] E. Sheha, H. S. Refai, *Electrochim. Acta* **2021**, *372*, 137883.
[35] M. Eckardt, D. Alwast, J. Schnaidt, R. J. Behm, *ChemSusChem* **2020**, *13*, 3919–3927.
[36] J. Ghilane, O. Fontaine, P. Martin, J.-C. Lacroix, H. Randriamahazaka, *Electrochem. Commun.* **2008**, *10*, 1205–1209.
[37] Z. Liu, O. Höfft, A. S. Gödde, F. Endres, *J. Phys. Chem. C* **2021**, *125*, 26793–26800.
[38] X. Gao, X. Liu, A. Mariani, G. A. Elia, M. Lechner, C. Streb, S. Passerini, *Energy Environ. Sci.* **2020**, *13*, 2559–2569.
[39] G. A. Giffin, A. Moretti, S. Jeong, K. Pilar, M. Brinkkötter, S. G. Greenbaum, M. Schönhoff, S. Passerini, *ChemSusChem* **2018**, *11*, 1981–1989.
[40] R. Lin, A. Ladshaw, Y. Nan, J. Liu, S. Yiacoumi, C. Tsouris, D. W. DePaoli, L. L. Tavlarides, *Ind. Eng. Chem. Res.* **2015**, *54*, 10442–10448.
[41] J. Čejka, G. Centi, J. Perez-Pariente, W. J. Roth, *Catal. Today* **2012**, *179*, 2–15.
[42] Y. Yan, T. Bein, *J. Am. Chem. Soc.* **1995**, *117*, 9990–9994.
[43] S. Rivera-Rubero, S. Baldelli, *J. Am. Chem. Soc.* **2004**, *126*, 11788–11789.
[44] K. A. Kurnia, T. E. Sintra, C. M. S. S. Neves, K. Shimizu, J. N. Canongia Lopes, F. Gonçalves, S. P. M. Ventura, M. G. Freire, L. M. N. B. F. Santos, J. A. P. Coutinho, *Phys. Chem. Chem. Phys.* **2014**, *16*, 19952.
[45] E. M. Flanigen, in *Studies in Surface Science and Catalysis* (Eds.: H. van Bekkum, E. M. Flanigen, J. C. Jansen), Elsevier, **1991**, pp. 13–34.
[46] P. Schatzberg, *J. Phys. Chem.* **1967**, *71*, 4569–4570.
[47] R. L. Gardas, H. F. Costa, M. G. Freire, P. J. Carvalho, I. M. Marrucho, I. M. A. Fonseca, A. G. M. Ferreira, J. A. P. Coutinho, *J. Chem. Eng. Data* **2008**, *53*, 805–811.
[48] M. M. Elnagar, J. M. Hermann, T. Jacob, L. A. Kibler, *Electrochim. Acta* **2021**, *372*, 137867.
[49] X. Hu, C. Chen, J. Yan, B. Mao, *J. Power Sources* **2015**, *293*, 187–195.
[50] R. Zarrougui, M. Dhahbi, D. Lemordan, *J. Electroanal. Chem.* **2014**, *717–718*, 189–195.
[51] M. M. Elnagar, T. Jacob, L. A. Kibler, *Electrochem. Sci. Adv.* **2022**, *2*, e2100175.
[52] P. C. Howlett, E. I. Izgorodina, M. Forsyth, D. R. MacFarlane, *Zeitschrift für Phys. Chemie* **2006**, *220*, 1483–1498.
[53] T. Pajkossy, C. Müller, T. Jacob, *Phys. Chem. Chem. Phys.* **2018**, *20*, 21241–21250.
[54] R. Wen, B. Rahn, O. M. Magnussen, *Angew. Chem. Int. Ed.* **2015**, *54*, 6062–6066.
[55] R. Atkin, S. Z. El Abedin, R. Hayes, L. H. S. Gasparotto, N. Borisenko, F. Endres, *J. Phys. Chem. C* **2009**, *113*, 13266–13272.
[56] B. Uhl, F. Buchner, D. Alwast, N. Wagner, R. J. Behm, *Beilstein J. Nanotechnol.* **2013**, *4*, 903–918.
[57] M. Brehm, H. Weber, A. S. Pensado, A. Stark, B. Kirchner, *Phys. Chem. Chem. Phys.* **2012**, *14*, 5030–5044.
[58] K. Motobayashi, M. Osawa, *Electrochem. Commun.* **2016**, *65*, 14–17.
[59] M. Gnahm, T. Pajkossy, D. M. Kolb, *Electrochim. Acta* **2010**, *55*, 6212–6217.
[60] T. Pajkossy, D. M. Kolb, *Electrochem. Commun.* **2011**, *13*, 284–286.
[61] M. Gnahm, C. Müller, R. Répánszki, T. Pajkossy, D. M. Kolb, *Phys. Chem. Chem. Phys.* **2011**, *13*, 11627.
[62] M. Gnahm, C. Berger, M. Arkhipova, H. Kunkel, T. Pajkossy, G. Maas, D. M. Kolb, *Phys. Chem. Chem. Phys.* **2012**, *14*, 10647.
[63] C. Müller, S. Vesztergom, T. Pajkossy, T. Jacob, *J. Electroanal. Chem.* **2015**, *737*, 218–225.
[64] C. Müller, S. Vesztergom, T. Pajkossy, T. Jacob, *Electrochim. Acta* **2016**, *188*, 512–515.
[65] C. Müller, K. Németh, S. Vesztergom, T. Pajkossy, T. Jacob, *Phys. Chem. Chem. Phys.* **2016**, *18*, 916–925.
[66] T. Pajkossy, C. Müller, T. Jacob, *Phys. Chem. Chem. Phys.* **2018**, *20*, 21241–21250.
[67] E. Anderson, V. Grozovski, L. Siinor, C. Siimenson, E. Lust, *J. Electroanal. Chem.* **2015**, *758*, 201–208.
[68] I. Weber, J. Ingenmey, J. Schnaidt, B. Kirchner, R. J. Behm, *ChemElectroChem* **2021**, *8*, 390–402.
[69] M. Kar, Z. Ma, L. M. Azofra, K. Chen, M. Forsyth, D. R. MacFarlane, *Chem. Commun.* **2016**, *52*, 4033–4036.
[70] G. Vardar, A. E. S. Sleightholme, J. Naruse, H. Hiramatsu, D. J. Siegel, C. W. Monroe, *ACS Appl. Mater. Interfaces* **2014**, *6*, 18033–18039.
[71] N. Sa, H. Wang, D. L. Proffit, A. L. Lipson, B. Key, M. Liu, Z. Feng, T. T. Fister, Y. Ren, C.-J. Sun, J. T. Vaughey, P. A. Fenter, K. A. Persson, A. K. Burrell, *J. Power Sources* **2016**, *323*, 44–50.
[72] Md. M. Islam, M. T. Alam, T. Okajima, T. Ohsaka, *J. Phys. Chem. C* **2009**, *113*, 3386–3389.
[73] M. Drüschler, B. Huber, S. Passerini, B. Roling, *J. Phys. Chem. C* **2010**, *114*, 3614–3617.

Manuscript received: March 22, 2023
Revised manuscript received: June 14, 2023
Accepted manuscript online: June 20, 2023
Version of record online: ■■, ■■

RESEARCH ARTICLE

This study deals with the fundamental understanding of the effect of trace amounts of water on the electrochemical properties of ionic liquids and their performance toward Mg deposition/dissolution.

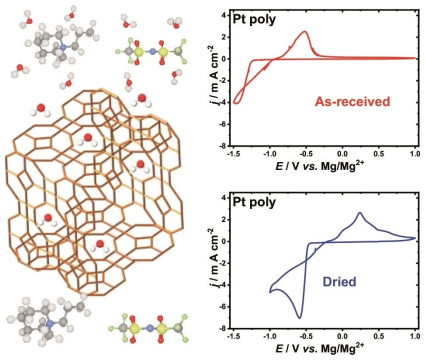

*O. W. Elkhafif, Dr. H. K. Hassan, Dr. M. U. Ceblin, Dr. A. Farkas, Prof. Dr. T. Jacob**